Surface Structure of Amyloid-β Fibrils Contributes to Cytotoxicity

Yuji Yoshiike,[‡] Takumi Akagi,[§] and Akihiko Takashima*[,‡]

Laboratory for Alzheimer's Disease, and Laboratory for Neural Architecture, RIKEN Brain Science Institute, Wako-shi, Saitama 351-0198, Japan

Received March 7, 2007; Revised Manuscript Received May 21, 2007

ABSTRACT: Amyloid β (Aβ) toxicity has been hypothesized to initiate the pathogenesis of Alzheimer's disease (AD). The characteristic fibrillar morphology of Aβ-aggregates, that constitute the main components of senile plaque, has long been considered to account for the neurotoxicity. But recent reports argue against a primary role for mature fibrils in AD pathogenesis because of the lack of a robust correlation between the severity of neurological impairment and the extent of amyloid deposition. Toxicity from the soluble prefibrillar intermediate entity of aggregates often called oligomer has recently proposed a plausible explanation for this inconsistency. An alternative explanation is based on the observation that certain amyloid fibril morphologies are more toxic than others, indicating that not all amyloid fibrils are equally toxic. Here, we report that it is not only the β-sheeted fibrillar structure but also the surface physicochemical composition that affects the toxicity of Aβ fibrils. For the first time, colloidal gold was used to visualize by electron microscopy positive-charge clusters on Aβ fibrils. Chemical modifications as well as point-mutated Aβ synthesis techniques were applied to change the surface structures of Aβ and to show how local structure affects surface properties that are responsible for electrostatic and hydrophobic interactions with cells. We also report that covering the surface of Aβ fibers with myelin basic protein, which has surface properties contrary to those of Aβ, suppresses Aβ toxicity. On the basis of these results, we propose that the surface structure of Aβ fibrils plays an important role in Aβ toxicity.

Alzheimer's disease (AD)[1] is characterized in pathological terms by senile plaques (SPs), neurofibrillary tangles (NFTs), and subsequent neuronal loss (*1*). Fibrillar aggregates of β-amyloid (Aβ) are a major component of SPs that take on a cross-β-pleated sheet conformation (i.e., β-aggregates) (*2*). β-aggregated Aβ is considered to be important in AD pathogenesis because it is toxic to cells (*3*).

Much effort has been exerted to understand the molecular basis of this toxic activity, but there is limited structural information about Aβ-aggregates that is directly related to toxic outcomes or effects (*4*−*7*). Acquiring information about the structure of Aβ at a higher resolution than has been achieved to date will likely reveal more clearly how structural characteristics contribute to Aβ function. Because of the aggregative nature of Aβ, crystallization of full-length Aβ has been unsuccessful. However, the crystal structure of a synthetic amyloid fibril of peptide fragment has been characterized (*8*). Although NMR techniques have greatly contributed to the 3D structural modeling of Aβ fibrils (*9*, *10*), demonstrating the parallel, in register β-sheet structure alone (*11*, *12*) does not fully explain the toxicity of Aβ fibrils. For example, more regular and longer fibrils tend to be more toxic (*7*, *12*). Certain amyloid fibril morphologies have been shown to be more toxic than others (*7*). Electrostatic interaction between Aβ fibrils with negatively charged membranes has been proposed to underlie the toxicity of Aβ toward neuronal cells (*13*, *14*). Interaction of hydrophobic sites of Aβ-aggregates with membrane has also been shown to induce a decrease in the membrane fluidity (*15*).

Taken together, this information led us to hypothesize that the cellular toxicity of Aβ fibrils is affected not only by the β-sheeted fibrillar structure but also by the physicochemical properties on the surface of β-aggregated Aβ fibrils. The attachment of negatively charged colloidal gold (CG) particles along Aβ fibers revealed the presence of positive-charge clusters on their surface. Experimental modification of this surface property through attenuation of the local Aβ structure reduced both CG attachment to fibers and Aβ toxicity. Conversely, maintenance of positive charges on fibrils upon fibril formation revealed a compound that counteracts toxicity, namely, myelin basic protein (MBP).

MATERIALS AND METHODS

Materials. Wild-type Aβ40 peptide was purchased from the Peptide Institute (Osaka, Japan). Triple mutant Aβ40 peptides, $(Ala)_3$ and $(M2k)_3$, were synthesized and purified as described previously (*16*). All other chemicals were purchased from Sigma-Aldrich (Saint Louis,) unless otherwise stated.

Aβ Fibril Preparation. To exclude the possibility that buffer molecules may complex with Aβ during chemical

* To whom correspondence should be addressed. Tel: +81-48-467-9627. Fax: +81-48-467-9627. E-mail: kenneth@brain.riken.jp.

[‡] Laboratory for Alzheimer's Disease.

[§] Laboratory for Neural Architecture.

[1] Abbreviations: AD, Alzheimer's disease; SP, senile plaque; Aβ, β-amyloid; MTT, 3-[4,5-dimethylthiazol-2-yl]-2,5-diphenyltetrazolium bromide; TEM, transmission electron microscopy; ThT, Thioflavin T; MBP, myelin basic protein; HFIP, 1,1,1,3,3,3-hexafluoroisopropanol; CG, colloidal gold; pLR, poly-L-Arg; $(Ala)_3$, Aβ40 (R5A, K16A, K28A) triple mutant; M2k, N^6,N^6-dimethyllysine; $(M2k)_3$, Aβ40 (R5M2k, K16M2k, K28M2k) triple mutant.

10.1021/bi700455c CCC: $37.00
Published on Web 08/04/2007

modification, lyophilized Aβ40 peptide (240 μM) was directly dissolved in cold 10% 1,1,1,3,3,3-hexafluoro-2-propanol (HFIP) solution and incubated at room temperature for 4 days under constant agitation in a siliconized tube covered with a lid containing holes. This incubation period was sufficiently long to evaporate off most, if not all, of the HFIP from solution because of its high vapor pressure. Extent of fibril formation was assessed by Thioflavin T (ThT) fluorescence intensity and by fibrillar morphology assessed by electron microscopy. In experiments using mutant Aβ peptides, three kinds of Aβ40, wild type, $(Ala)_3$, and $(M2k)_3$, were dissolved in HFIP then aliquoted and frozen at −80 °C until use. Aliquots were vacuum-centrifuged using a Savant Speed-vac system (Holbrook,) until most HFIP evaporated. Just prior to complete desiccation, the peptides were dissolved in 20 mM Tris-HCl (pH 7.4) on ice. Three peptide solutions (10 μM each) and buffer alone were incubated in siliconized tubes at 37 °C for 212 h without agitation.

Transmission Electron Microscopy (TEM). Five microliters of each sample was applied to Formvar-coated 300-mesh copper or nickel grids. Aβ fibrils were co-incubated with 5 nm colloidal gold (CG) (Sigma-Aldrich) (0.01% as $HAuCl_4$) for 1 h and then fixed with 5% glutaraldehyde solution in 50 mM sodium phosphate buffer (pH 7.4). After staining the preparations with 1% (w/v) neutralized tungstophosphate or with 1% (w/v) uranyl acetate, the grids were examined on a LEO 912AB electron microscope at an accelerating voltage of 100 kV or on a CM20 electron microscope at 80 kV.

Cell Viability Assay. Human embryonic kidney (HEK) 293 cells were used to test the toxic effects of various samples as assessed in the 3-[4,5-dimethylthiazol-2-yl]-2,5-diphenyltetrazolium bromide (MTT) assay. Cells were grown in Dulbecco's modified Eagle's medium (DMEM) containing 10% fetal bovine serum and incubated in a humidified chamber (85% humidity) containing 5% CO_2 at 37 °C. Two days before peptide sample treatment, the cell culture medium was replaced with serum-free DMEM, and the cells were trypsinized and re-plated onto coated 96-well plates at a final cell density of 20,000 cells/well. Two hours after the cells were incubated with peptide samples, MTT was added to each well, and the plates were kept in a CO_2 incubator for an additional 2 h. The cells were then lysed by adding lysis solution (50% dimethylformamide, 20% SDS at pH 4.7) and were incubated overnight. The degree of MTT reduction (i.e., cell viability) in each sample was subsequently assessed by measuring absorption at 550 nm at 37 °C using a plate reader. Background absorbance values, as assessed from cell-free wells, were subtracted from the absorption values of each test sample. The absorbance measured from the three wells were averaged, and the percentage MTT reduction was calculated by dividing this average by the absorbance measured from a control sample lacking peptide sample.

Thioflavin T (ThT) Assay. The degree of β-aggregation was determined using the fluorescent dye, ThT, which specifically binds to β-aggregated structures (*17*). Measurements were performed at excitation and emission wavelengths of 444 and 485 nm, respectively, wavelengths that result in the optimum detection of bound ThT. To account for background fluorescence, the fluorescence intensity measured from each control solution (i.e., lacking Aβ fibril sample) was subtracted from that of each solution containing the sample. Measurements were obtained in triplicate.

Chemical Modifications (Glycation and Acetylation). Samples of preformed Aβ fibers (120 μM in H_2O) and H_2O (control) were incubated with glucose (1 M in H_2O), aspirin (0.5 M in H_2O), or H_2O at 100 °C for 4 h. Thus, H_2O-treated Aβ fibers were also heat-treated. Lids of tubes containing samples were tightly taped to avoid evaporation as much as possible. For the same purpose, tubes were incubated in a humidified oven. After heat treatment, the pH and volume of each sample were adjusted to neutral and to the volume prior to treatment, respectively. Glucose and aspirin were not removed from each solution after the treatment. In the following three assays (i.e., ThT, ninhydrin, and MTT), we compared results between the Aβ sample treated with glucose, aspirin, or H_2O and each control, namely, glucose, aspirin, or H_2O alone without Aβ. The extent of Aβ modification was assessed by ninhydrin assay, which easily measures the amount of free amines. Each sample was blotted onto silica plates, then premixed ninhydrin assay solution was poured over the plates. After drying the plates with heat, the plates were scanned three times to quantify the intensity of the ninhydrin blue reaction product, which appears as blue dots. A blue reaction product indicates the presence of free amines in a sample.

Sedimentation Assay (OD214). To account for the different affinity of ThT for different amino acid residues, we performed a sedimentation assay to adjust the mass concentration of aggregates prepared from mutant Aβ peptides, as described previously (*18*). This ensured that cell cultures tested with the MTT assay were exposed to comparable amounts of aggregates. We used the following equation to calculate the mass concentration of the aggregates we used for the MTT assay: 10% mass concentration of aggregates = 10% × (mass concentration of aggregates) ÷ (percentage of aggregation). Regrettably, this method of sedimentation assay was not suitable for determining the level of aggregation in chemical modification experiments since both glucose and aspirin interfered significantly with the absorbance readings. However, ThT assay results with EM pictures showed that substantial amount of fibrils remained intact. ThT fluorescence measurements indicated that heat-treated Aβ fibrils in the presence of glucose or aspirin had higher β-aggregation levels than did heat-treated Aβ fibrils in the absence of glucose or aspirin. Aβ fibrils heat-treated in H_2O without glucose or aspirin still showed a significantly higher fluorescence level than the control (i.e., H_2O without Aβ).

Trp Fluorescence. Intrinsic fluorescence emission by the Trp residue in myelin basic protein (MBP) was measured to monitor its interaction with Aβ fibers (*19*). Since the Trp residue of MBP is excited at 295 nm, we measured the emission spectra between 300 to 400 nm; emission values at 364 nm were taken as maxima.

RESULTS

Detection of Positive-Charge Clusters on Aβ Aggregates. The charge-based interaction of Aβ peptide with cell membranes has been previously proposed (*20*). There is also consensus in the literature that electrostatics play a role in Aβ interactions with negatively charged lipids (*13*, *14*). Yet, the electrostatic properties of aggregated Aβ have never been

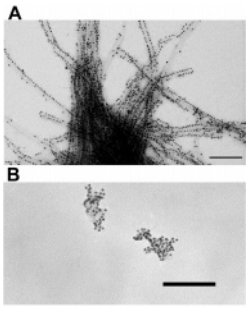

FIGURE 1: Visualization of positive charge-clusters. (A) Aβ40 (10 μM) was incubated in 5 mM HEPES (pH 7.4) and 0.9% NaCl at 37 °C until the level of β-aggregation reached a plateau; β-aggregation was monitored by ThT fluorescence (*17*). The aggregated Aβ sample was then treated with CG (5 nm particle size) solution for another hour and applied to Formvar-coated 300-mesh copper grids. The grids were then stained with 1% (w/v) neutralized tungstophosphoric acid. The specimen was examined on an LEO 912AB electron microscope at an accelerating voltage of 100 kV. Magnification is 80,000, and the scale bar is 100 nm. (B) Freshly dissolved 23 μM pLR (average MW, 40 kDa) in H_2O was co-incubated with CG at room temperature, dropped onto nickel grids, and then negatively stained with 1% (w/v) uranyl acetate. The specimen was examined on a CM20 electron microscope at an accelerating voltage of 80 kV. Magnification is 66,000, and the scale bar is 50 nm.

directly observed on the surface of fibrils, presumably because conventional techniques that can render these data at above molecular resolution, such as crystallography, have been challenging in studies on amyloid.

In the present study, we used CG to locate positively charged sites along Aβ fibers. Each CG nanoparticle is composed of a crystalline gold core surrounded by an ionic double layer shell (*21*). The inner layer of this shell is made from absorbed gold dichloride ions and the outer layer is made from diffuse hydrogen ions, giving each CG particle an overall negative surface charge (*21*). Therefore, the positive charges along Aβ fibers should attract CG, enabling us to map the distribution of positive charges on these fibers by transmission electron microscopy (TEM). Indeed, we observed a great number of CG particles attached to Aβ fibers (Figure 1A). Although CG adhesion was almost continuous along the fibers, CG coverage was not complete. CG particles tended to align along one or two sides of a fiber, indicating that clusters of positive charges exist along Aβ fibers. To ensure the electrostatic interactions between the negative charges on CG particles and the positive charges on peptides, we performed an internal control experiment by incubating CG with polymers of positively charged arginine amino acids (poly-L-Arg; pLR) (Figure 1B). We observed significant binding of CG particles onto the amorphous mass of pLR, confirming an electrostatic interaction between CG and basic amino acids. Although Aβ fibers and pLRs have completely different structures, they both possess clustered positive charges on their surfaces. Importantly, both of them are cytotoxic (*4*−*7*, *22*).

Charge Balance in Aβ Aggregation and Toxicity. The net charge of Aβ at physiological pH is about −3. Thus, a notable characteristic of Aβ-aggregation is the formation of positive-charge clusters without the corresponding neutralization of positive charges by negative charges. It is possible that a charge balance on the Aβ peptides may have helped make this process possible and that disrupting that balance

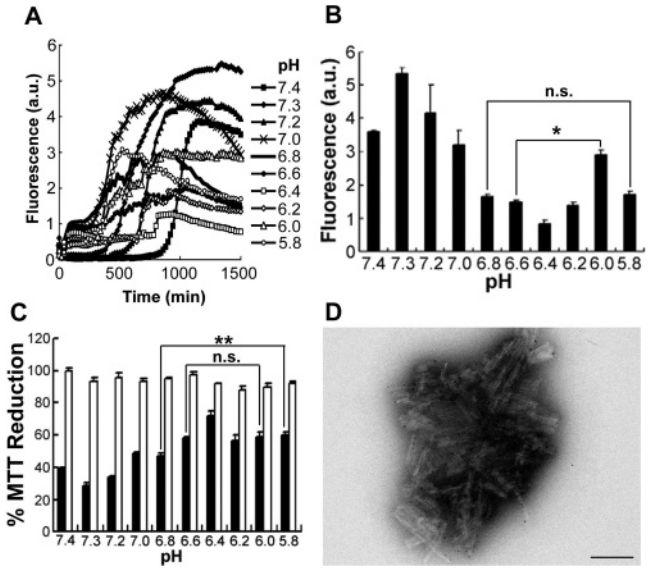

FIGURE 2: Balance of charge in Aβ-aggregation and toxicity. (A) Aβ40 (5 μM) was pretreated with HFIP and was incubated at 37 °C with 10 μM ThT in 5 mM HEPES at the series of pH values shown in the panel. The relative degree of β-aggregation was assessed in terms of fluorescence intensity. To account for background fluorescence, the fluorescence intensity measured from each control solution without Aβ was subtracted from that of each solution containing Aβ. (B) Fluorescence intensity of each sample after 25 h of incubation. Statistical significance was calculated by using Student's *t*-test; * $p < 0.05$; n.s. = not significant. (C) Samples from the incubation well added to HEK 293 cell cultures and assayed for cytotoxicity at a final concentration of 420 nM Aβ40 (filled bars) and water (open bars) with MTT reduction (i.e., cell viability). The absorbance (570 nm) value from water at pH 7.4 was 100%. Statistical significance was calculated by using Student's *t*-test; ** $p < 0.01$; n.s. = not significant. Note that despite the significantly higher β-aggregation level of the pH 6.0 sample compared to that of the pH 6.6 sample, there was no difference in their toxicity. Also note that despite the lack of significant difference in the β-aggregation level between the pH 5.8 and pH 6.8 samples, the pH 5.8 sample was significantly less toxic than the pH 6.8 sample. (D) Aβ40-aggregates that formed at pH 5.8 and incubated with CG were applied to copper grids. After fixation by 5% glutaraldehyde solution, they were stained with 1% neutralized tungstophosphoric acid. Magnification is 80,000, and the scale bars are 100 nm.

would influence the β-aggregation and, consequently, Aβ toxicity. The pH dependency of Aβ-aggregation kinetics was monitored by ThT fluorescence assay (Figure 2A). pH ranges from 7.4 to 5.8 had two peaks of β-aggregation using Aβ40 (Figure 2B). The first peak was observed at pH 7.3, within the physiological range of pH reduction in acidosis (*23*). We speculated that a slight increase in positive charges within the Aβ sequence through the protonation among three histidine residues inducing nucleation by the electrostatic interactions between side chains may explain this phenomenon. A lower level of β-aggregation was reached at lower pH (pH 7.2−6.4) presumably because the highly increased positive charges induced the nucleation process so effectively that it suppressed the elongation process (Figure 2A). The overinducing effect of nucleation decreased at even lower pH, and a second peak of β-aggregation was observed at pH 6.0 (Figure 2B). Interestingly, while the extent of β-aggregation correlated well with toxicity in the pH range from 7.4 to 6.2, it did not with the two samples formed at pH 6.0 and pH 5.8 (Figure 2B and C). Despite the high level of β-aggregation at pH 6.0 that is almost twice the level at

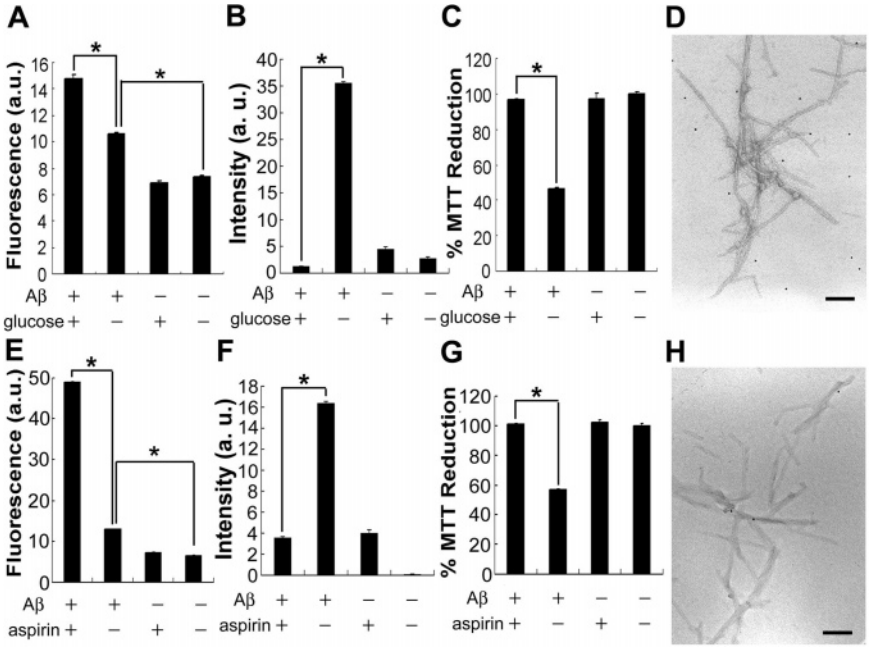

FIGURE 3: Effects of chemically modified positive charges on Aβ-toxicity. (A) β-aggregation of glycated Aβ. Aβ fibrils and H_2O in the presence or absence of glucose were heat-treated. Each sample (Aβ fibrils treated with glucose, Aβ fibrils treated with H_2O, glucose alone without Aβ, and H_2O alone without Aβ) was mixed with 25 μM ThT, and β-aggregation was monitored by measuring fluorescence. (B) Effect of glycation on Aβ-associated amines. Ninhydrin assay was performed on 2.5 μL of four samples (glucose-treated Aβ fibrils, H_2O-treated Aβ fibrils, glucose alone, and H_2O alone). (C) Effect of glycation on Aβ-related cytotoxicity. Four samples were diluted and added to HEK 293 cell cultures for MTT assay. Final concentration of Aβ40 was 120 nM. (D) Effect of glycation on positive-charge clusters of Aβ fibers. Glucose-treated Aβ fibers were co-incubated with CG and observed under TEM. Aβ fibrils and H_2O in the presence or absence of aspirin were heat-treated. The ThT fluorescence (E) ninhydrin reactivity (F), and cytotoxicity (G) of four samples (Aβ fibrils treated with aspirin, Aβ fibrils treated with H_2O, aspirin alone without Aβ, and H_2O alone without Aβ) were assessed as described for A−C. (H) Effect of acetylation on positive-charge clusters of Aβ fibers. Acetylated Aβ fiber was co-incubated with CG and observed under TEM. D and H were examined on a CM20 electron microscope at 80 kV. Magnification is 66,000, and the scale bars are 100 nm. Statistical significance was calculated by using a Student's *t*-test; $*p < 0.001$. Data are presented as means of triplicates ± SEM.

pH 6.6, there was no significant difference in the toxicity between two samples prepared at pH 6.0 and pH 6.6 (Figure 2B and C). Because the isoelectric point (pI) of Aβ40 is around 5.8, the second peak of aggregation at pH 6.0 may follow the general principle of proteins to aggregate and precipitate out of solution when their net charge reaches zero. Aggregates formed at pH 5.8 were shorter, had greater affinity to cluster together, and showed fewer CG adhesions (Figure 2D). The electrostatic attractions of Aβ peptides at its pI caused the clumping or bundling of short fibers and suppressed the formation of exposed positive-charge clusters, resulting in lower than expected toxicity. This phenomenon is consistent with and supports a report showing that Aβ fibrils formed with agitation exhibited higher tendency to associate laterally, thus forming bundles and having a lower toxicity than Aβ fibrils formed without agitation (*7*). Therefore, the positive charge balance of Aβ peptides directly influences the β-aggregation process in forming positive-charge clusters and affects toxicity.

Contribution of Positive-Charge Clusters to Aβ Toxicity. To investigate how positive-charge clusters contribute to the toxicity of Aβ-aggregates, we chemically modified preformed Aβ fibers by glycation and acetylation. Both methods modify positively charged sites in proteins (*24*−*27*). Changes in β-aggregation through glycation were monitored by measuring Thioflavin T (ThT) fluorescence (*17*). We found that Aβ fibers treated with glucose had higher β-aggregation levels than did Aβ fibers treated with H_2O, whose β-aggregation level was still significantly high (Figure 3A). Loss of ninhydrin reactivity indicated that the glycated Aβ had lost positive charges in its amino group (Figure 3B). Interestingly, glycated Aβ fibers had almost no toxic activity at the final concentration tested (120 nM) (Figure 3C).

Next, we co-incubated glycated Aβ fibers with CG, examined them with TEM, and found that the fibrous structure of the glycated fibers remained intact, even though adhesion was minimal (Figure 3D). These results suggested that glycation suppressed toxicity by reducing the positive charges on Aβ fibers. Similar results were obtained when Aβ fibers were treated with aspirin (Figure 3E−H), an acetylating agent (*26*, *27*) known to reduce the risk of AD (*28*). Aβ fibers treated with aspirin showed much greater levels of β-aggregation, as assessed by ThT fluorescence, than did H_2O-treated Aβ fibers (Figure 3E). By contrast, our ninhydrin and MTT assay results showed that toxicity declined as aspirin-related acetylation reduced positive charges of the Aβ fibers (Figure 3F and G). TEM examination of aspirin-treated Aβ revealed that the fibrous structure of the fibers remained intact (Figure 3H).

The toxicity of Aβ fibers was not reduced simply by addition of glucose or aspirin at the concentration used (data not shown); the Aβ and glucose or aspirin mixture had to be heat treated to induce chemical modification of Aβ fibers before assaying toxicity on cells. These results from the glycation and acetylation experiments suggest that positive-charge clusters play an important role in Aβ toxicity, even though it is unknown how the local structural change caused by these modifications might have affected toxicity.

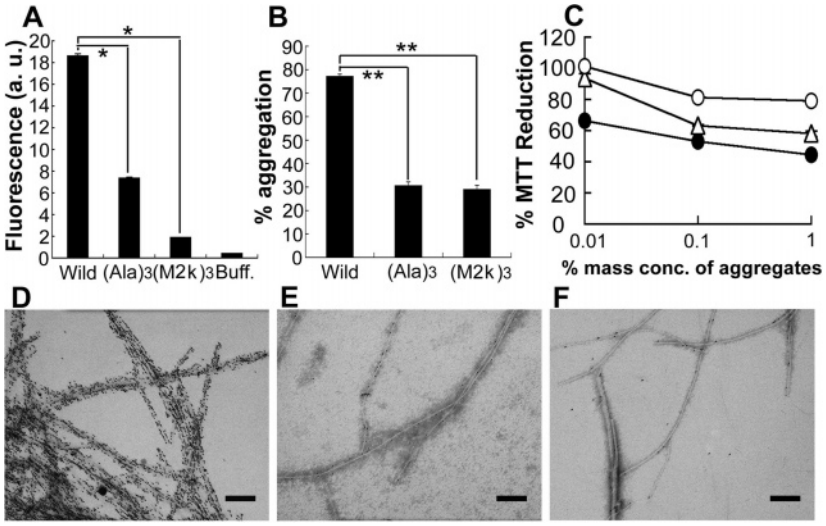

FIGURE 4: Modification of local structure affects Aβ surface properties and toxicity. (A) β-aggregation of wild-type and mutant Aβ as assessed by ThT fluorescence. Wild-type Aβ and two Aβ mutants, $(Ala)_3$ and $(M2k)_3$, were dissolved in 20 mM Tris-HCl (pH 7.4) to a final concentration of 10 μM and incubated at 37 °C for 212 h. $(Ala)_3$ and $(M2k)_3$ are synthetic Aβ40 peptides whose three basic residues (Arg5, Lys16, and Lys28) are mutated to Ala and M2k residues, respectively. M2k is N^6,N^6-dimethyllysine. The fluorescence intensity of each sample, including buffer alone, was measured by ThT (final concentration, 10 μM). Statistical significance was calculated by using a Student's *t*-test, $*p < 0.0005$. Data are presented as means of triplicates ± SEM. (B) Percent aggregation of each sample assessed by measuring absorbance at a wavelength of 214 nm, as described in Materials and Methods. $**p < 0.001$. (C) Effect of Aβ mutation on cytotoxicity. The percent mass concentration of aggregates in each Aβ sample was adjusted, and cytotoxicity was assessed by MTT assay. The Aβ samples were added to HEK293 cells cultured in 50% serum-free DMEM, and after 22 h, MTT was added to the cells, which were incubated further for 2 h ($n = 3$). Cytotoxic effects by three kinds of Aβ fibrils (wild type (●), $(Ala)_3$ (△), and $(M2k)_3$ (○)) are significantly different by two-way ANOVA: $p < 0.0001$. (D−F) Amino acid mutations affect Aβ surface characteristics. Wild-type Aβ fibers (D) $(Ala)_3$ Aβ fibers (E), and $(M2k)_3$ Aβ fibers (F) were co-incubated with CG (5 nm) at room temperature, applied onto nickel grids, fixed with 5% glutaraldehyde solution, then negatively stained with 2% phosphotungstate (pH 7.1). Grids were examined on an LEO912AB electron microscope at 100 kV. Magnification is 80,000, and the scale bars are 100 nm.

Local Structures Affect the Surface Properties of Aβ Fibrils and Their Cytotoxicity. To determine the role that local surface structures play in Aβ toxicity, we assessed the β-aggregation capacity and cytotoxicity of two mutant Aβ peptides. One mutant, $(Ala)_3$, is a point mutant (R5A, K16A, K28A) of Aβ40 in which three basic residues were replaced with hydrophobic Ala residues, and the other mutant, $(M2k)_3$, is a point mutant (R5M2k, K16M2k, K28M2k) of Aβ40 in which the three basic residues of wild-type Aβ were replaced with less hydrophobic N^6,N^6-dimethyllysines (M2k).

After incubating samples of wild-type Aβ and the two Aβ mutants for the same period under the same conditions, we assessed the extent of β-aggregation by measuring ThT fluorescence (Figure 4A). Both $(Ala)_3$ and $(M2k)_3$ showed less β-aggregation than did the wild type. Since ThT may bind peptides having different sequences with varying affinity, we also assessed aggregation by adjusting the concentration of aggregates and measuring the percentage of aggregation by sedimentation assay (Figure 4B). Consistent with our ThT results, both the $(Ala)_3$ and $(M2k)_3$ mutants showed a significantly lower percentage of aggregation than did wild-type Aβ (Figure 4B).

Next, we assessed and compared the cytotoxicity of Aβ-aggregates formed by each Aβ mutant to those formed by wild-type Aβ by using an MTT assay. To ensure that cell cultures were exposed to comparable amounts of aggregates, we used the percentage of aggregation values to calculate the percentage of mass concentration for each type of Aβ-aggregate. Aggregates of the $(Ala)_3$ mutant showed slightly but significantly lower toxicity than did those of wild-type Aβ (Figure 4C), although the difference was not as large as that expected from the chemical modification experiments. Contrary to our expectation, positively charged $(M2k)_3$ aggregates showed much lower toxicity than did wild-type Aβ-aggregates, even more significantly than $(Ala)_3$ (Figure 4C). The $(Ala)_3$ toxicity we observed may be due to the remaining positive charges stemming from His residues, whose subpopulation remains positively charged at neutral pH. This possibility is consistent with the pattern of CG binding on $(Ala)_3$ fibrils, even though much fewer CG particles bound to the mutant than to wild-type Aβ fibrils (Figure 4D and E).

Alternatively, $(Ala)_3$ toxicity may also be due to the hydrophobicity of the mutant because the interaction between hydrophobic sites on Aβ-aggregates and membrane has also been suggested previously (*15*). Then, positive-charge clusters alone do not affect on Aβ toxicity. Ala has a hydrophobicity of 0.616, whereas Arg and Lys have hydrophobicities of 0.000 and 0.283, respectively (*29*). Although it is almost impossible to remove positive charges without altering the surface properties on Aβ fibrils, the overall hydrophobicity of fibrils can be maintained at a more or less constant level, as with $(M2k)_3$ mutant fibrils. To create $(M2k)_3$, the three basic residues of wild-type Aβ were replaced with N^6,N^6-dimethyllysine (M2k), which has a hydrophobicity of 0.151 in contrast to 0.189, the average hydrophobicity of one Arg and two Lys. The reason for such a low hydrophobicity for M2k is that M2k remains positively charged, as found with heterochromatin-associated protein 1 (HP1) (*30*).

Comparing aggregates formed by $(M2k)_3$ and wild-type Aβ enabled us to study how local surface structure can contribute to Aβ fibril toxicity (Figure 4). Although both $(M2k)_3$ and wild-type Aβ are positively charged and have comparable hydrophobicities, $(M2k)_3$ aggregates were much

less toxic than were wild-type aggregates (Figure 4C). This result can be explained by analogy to HP1, whose methylated lysine side chain is unsuitable for "normal" electrostatic interactions (*30*). This is because methylation of lysine N^{ζ} adds hydrophobic methyl groups and polarizes the $N^{\zeta}-C^{\epsilon}$ bond, creating a delocalized positive charge that prefers cation$-\pi$ interactions with aromatic residues (*31*). This property of the M2k residue, whose delocalized positive charge is not suitable for electrostatic interactions, is reflected qualitatively in the reduced CG binding we observed on $(M2k)_3$ mutant Aβ fibers (Figure 4F). This finding suggests that it is not simply the positive-charge clusters but the local structure that affects surface physicochemical composition of Aβ fibrils responsible for various interactions with cell membranes.

Collectively, these results suggest that surface physicochemical composition contributes significantly to Aβ toxicity and their efficacy depends largely on the local structures of amino acid side chains.

Inhibition of Aβ Toxicity on the Basis of the Surface Properties of Aβ Aggregates. Thus far, we have considered the effects of surface physicochemical properties of Aβ-aggregates on toxicity. Then, we searched for a compound that would reasonably inhibit the surface properties of Aβ fibers, suppressing or at least reducing, their toxicity. If electrostatic interactions between positive-charge clusters and negatively charged cell membranes induce toxicity, then to reduce toxicity, these positive charges would need to be neutralized by negative charges. However, because Aβ possesses a net negative charge at physiological pH, we needed to identify a compound with positive charges to enhance interactions with the negatively charged sites on Aβ fibrils. Since the positive charges of Aβ-aggregates remain intact, we assumed that the positive-to-negative charge ratio of wild-type Aβ peptide within the amyloid structure that is almost 1:2 at physiological pH may also remain the same or at least may remain similar to that of Aβ monomers. Therefore, we looked for compounds that possess more positive charges than negative charges, particularly those with a positive-to-negative charge ratio close to 2:1, which is the reciprocal of the charge ratio of monomeric Aβ. At the same time, these compounds should also possess some hydrophobic amino acids, which would ideally interact with the hydrophobic sites on Aβ fibers.

We found MBP to be a molecule with properties closely matching the above requirements. The positive-to-negative charge ratio of bovine MBP is ~3:1, and ~46% of its sequence consists of hydrophobic amino acids. Because MBP has one Trp residue and Aβ has none, we monitored Trp fluorescence to assess the interaction of MBP with Aβ fibers (Figure 5A). Fluorescence emission maxima increased with increasing Aβ concentrations, suggesting that MBP and Aβ fibers interacted (*19*).

To determine whether this interaction largely depends upon electrostatic associations, we treated samples containing MBP and Aβ fibers with salt (Figure 5B). The presence of 1 M NaCl reduced the emission maximum to control levels (i.e., that of samples containing MBP and salt). Although how MBP exactly interacts with Aβ fibers is unknown; this observation indicates that electrostatic interactions between Aβ and MBP did indeed occur.

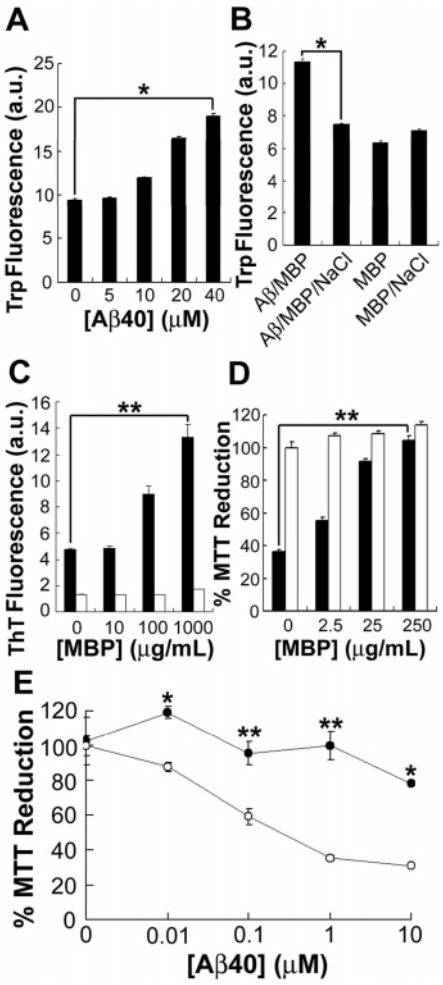

FIGURE 5: Inhibition of Aβ-toxicity by MBP. (A) Interaction of MBP with Aβ fibers. Aβ40 fiber solutions at the concentrations indicated were mixed with 10 μM bovine MBP (MW, 18.4 kDa), and MBP binding to Aβ was assessed by monitoring Trp fluorescence. (B) Effect of salts on MBP$-$Aβ fiber interactions. Trp fluorescence measurements were performed on samples containing 10 μM MBP with or without 20 μM Aβ40 fiber and 1 M NaCl. (C) Effect of MBP on Aβ-aggregation. β-aggregation of samples containing various concentrations of MBP and either 10 μM preincubated Aβ40 (filled bars) or H_2O (open bars) was measured by monitoring ThT fluorescence. (D) Effect of MBP on Aβ cytotoxicity. We used the MTT assay to measure the toxicity of Aβ fibers (final concentration of 1 μM Aβ40) in the presence of MBP. Filled bars, with Aβ; open bars, without Aβ. (E) Concentration-dependent toxicity of Aβ40 fiber measured by MTT assay in the presence (●) and the absence (○) of 50 μg/mL MBP; $n = 3$; $^{*}p < 0.005$; and $^{**}p < 0.05$.

Next, we examined whether MBP affects the aggregation and cytotoxicity of Aβ fibers. ThT assay of samples containing both MBP and preformed Aβ fibers showed increased β-aggregation with increasing MBP concentrations (Figure 5C). MTT assay of cells treated with these samples revealed that MBP inhibited the toxicity of Aβ fibers (Figure 5D). Moreover, the dose-dependent toxicity of Aβ fibers was clearly suppressed by MBP (Figure 5E). These results suggest that MBP inhibits Aβ toxicity by inhibiting the surface activity of Aβ fibers through electrostatic interactions. From these results, we propose that the toxicity of Aβ fibrils is significantly affected by the surface physicochemical structure despite the detailed mechanism, and which specific surface properties is yet unknown.

DISCUSSION

Aβ generation and associated conformational changes into the cross-β-pleated sheet amyloid structure (*2*) observed in SPs are hypothesized to initiate the pathogenesis of AD (*1*). Although Aβ toxicity depends on its aggregation state and on the electrostatic interaction with cells (*13*, *14*, *20*), the mechanism of that toxicity remains unknown because detailed structural knowledge is lacking (*12*, *19*). Using CG, we investigated the positively charged surface properties of Aβ-aggregates and how they contribute to Aβ toxicity. The presence of positive-charge clusters implies that systematic β-aggregation results in clustering of surface physicochemical properties. This is indeed consistent with the parallel, in register β-sheet 3D model of Aβ fibers (*7*, *11*, *12*) that predicts clustering of the physicochemical properties of side chains on the surface of Aβ fibers. Although we also attempted to locate the negatively charged surface properties by using cationic CG, we were unable to observe its adhesion on Aβ fibers, most likely because of the contamination of pLK in cationic CG solution. Thus far, the technique of CG attachment to investigate surface properties is limited to a qualitative analysis. Technical improvement in the future should allow for more quantitative analysis of surface structure on a protein or on a macromolecular protein complex of nanoscale.

We observed that Aβ-aggregates formed at pH close to the pI of Aβ were clumped and showed fewer CG adhesions, resulting in lower than expected toxicity from the extent of β-aggregation. We also observed that chemical modifications of basic residues inhibited the toxicity of fibrillar Aβ and decreased CG attachment, suggesting that positive-charge clusters may play a significant role in wild type Aβ fiber toxicity. We also investigated how local surface structure contributed to the cytotoxicity of Aβ fibers. We found that a triple-Ala mutant of Aβ was slightly but significantly less toxic than wild-type Aβ, a finding that supports the importance of positive-charge clusters on the toxicity of wild Aβ fibrils and at the same time, as suggested previously (*15*), the possible involvement of increased hydrophobicity (from Ala) in decreasing the toxicity of these more hydrophobic mutant Aβ fibrils. M2k was used to examine these surface properties of Aβ-aggregates in more detail. Analysis of a $(M2k)_3$ mutant of Aβ suggested that the local structure of amino acid residues, which greatly affects the availability of the molecule surface for electrostatic interaction, thus not the positive charge alone, plays a significant role in the interaction between Aβ fibers and cells and the subsequent toxicity.

The observation of positive-charge clusters on Aβ fibers also suggested the partial, if not complete, preservation of surface physicochemical properties of Aβ after systematic β-aggregation. Using the structural characteristics of monomeric Aβ as a guide, we searched for a molecule with a reciprocal charge ratio and moderate hydrophobicity to counteract and inhibit the surface activities of Aβ fibers. MBP proved to be an effective inhibitor of Aβ toxicity, even though an application of MBP for a therapeutic purpose may not be appropriate since MBP induces autoimmune encephalomyletis. Nonetheless, this result indirectly supports our hypothesis that surface physicochemical structure composed of the side chains of systematic β-aggregates plays an important role in Aβ toxicity. Moreover, our findings collectively explain the structure−toxicity relationship of Aβ fibrils. Upon its formation, the parallel, in register β-sheet structure of Aβ fibers should cause the clustering the physicochemical properties of at least some side chains. We speculate here that these clusters on the surface of Aβ fibers induce toxicity. Because this toxic clustering of surface properties occurs as a result of systematic β-aggregation, more regular and longer Aβ fibrils tend to become more toxic (*7*, *12*). This observation supports the concept that neuronal degeneration in AD is caused by the deposition of β amyloid (*1*, *32*).

However, there are also arguments against a primary role for mature fibrils in AD pathogenesis. They are mostly based on the absence of a robust correlation between the severity of neurological impairment and the extent of amyloid deposition (*4*, *33*, *34*). Our results that modified surface properties of Aβ by fiber bundling, chemical modifications, synthetic point mutagenesis, and interaction with MBP all consistently show that the extent of β-aggregation is not perfectly correlated with toxicity. Instead, our results suggest that it is not just the β-sheeted fibrillar structure but also the surface physicochemical composition that affects the toxicity of Aβ fibrils in ways that we still do not understand. In relation to this, certain amyloid fibril morphologies have been shown to be more toxic than others (*7*). Therefore, we propose that alteration of the surface properties of Aβ fibrils such as fiber bundling, post-translational modifications, or interactions with other molecules possibly weakens the correlation between disease symptom and amyloid deposition.

ACKNOWLEDGMENT

We thank Dr. Charles G. Glabe and his colleagues for great advice and support.

REFERENCES

1. Selkoe, D. J. (2004) Cell biology of protein misfolding: the examples of Alzheimer's and Parkinson's diseases, *Nat. Cell Biol. 6*, 1054−1061.
2. Sunde, M., and Blake, C. C. F. (1998) From the globular to the fibrous state: protein structure and structural conversion in amyloid formation, *Q. Rev. Biophys. 31*, 1−39.
3. Pike, C. J., Burdick, D., Walencewicz, A. J., Glabe, C. G., and Cotman, C. W. (1993) Neurodegeneration induced by beta-amyloid peptides in vitro: the role of peptide assembly state, *J. Neurosci. 13*, 1676−1687.
4. Mandelkow, E. (2000) bAPtism, *Cell 101*, 139−141.
5. Lashuel, H. A., Hartley, D., Petre, B. M., Walz, T., and Lansbury, P. T., Jr (2002) Neurodegenerative disease: amyloid pores from pathogenic mutations, *Nature 418*, 291.
6. Kayed, R., Head, E., Thompson, J. L., McIntire, T. M., Milton, S. C., Cotman, C. W., and Glabe, C. G. (2003) Common structure of soluble amyloid oligomers implies common mechanism of pathogenesis, *Science 300*, 468−469.
7. Petkova, A. T., Leapman, R. D., Guo, Z., Yau, W. M., Mattson, M. P., and Tycko, R. (2005) Self-propagating, molecular-level polymorphism in Alzheimer's beta-amyloid fibrils, *Science 307*, 262−265.
8. Nelson, R., Sawaya, M. R., Balbirnie, M., Madison, A. O., Riekel, C., Grothe, R., and Eisenberg, D. (2005) Structure of the cross-beta spine of amyloid-like fibrils, *Nature 435*, 773−778.
9. Tycko, R. (2004) Progress towards a molecular-level structural understanding of amyloid fibrils, *Curr. Opin. Struct. Biol. 14*, 96−103.

10. Ritter, C., Maddelein, M. L., Siemer, A. B., Luhrs, T., Ernst, M., Meier, B. H., Saupe, S. J., and Riek, R. (2005) Correlation of structural elements and infectivity of the HET-s prion, *Nature 435*, 844−848.
11. Balbach, J. J., Petkova, A. T., Oyler, N. A., Antzutkin, O. N., Gordon, D. J., Meredith, S. C., and Tycko, R. (2002) Supramolecular structure in full-length Alzheimer's beta-amyloid fibrils: evidence for a parallel beta-sheet organization from solid-state nuclear magnetic resonance, *Biophys. J. 83*, 1205−1216.
12. Luhrs, T., Ritter, C., Adrian, M., Riek-Loher, D., Bohrmann, B., Dobeli, H., Schubert, D., and Riek, R. (2005) 3D structure of Alzheimer's amyloid-beta(1−42) fibrils, *Proc. Natl. Acad. Sci. U.S.A. 102*, 17342−17347.
13. Terzi, E., Holzemann, G., and Seelig, J. (1994) Alzheimer beta-amyloid peptide 25−35: electrostatic interactions with phospholipid membranes, *Biochemistry 33*, 7434−7441.
14. Vargas, J., Alarcon, J. M., and Rojas, E. (2000) Displacement currents associated with the insertion of Alzheimer disease amyloid beta-peptide into planar bilayer membranes, *Biophys. J. 79*, 934−944.
15. Kremer, J. J., Pallitto, M. M., Sklansky, D. J., and Murphy, R. M. (2000) Correlation of beta-amyloid aggregate size and hydrophobicity with decreased bilayer fluidity of model membranes. *Biochemistry 39*, 10309−10318.
16. Yoshiike, Y., Chui, D. H., Akagi, T., Tanaka, N., and Takashima, A. (2003) Specific compositions of amyloid-β peptides as the determinant of toxic β-aggregation, *J. Biol. Chem. 278*, 23648−23655.
17. LeVine, H. III (1993) Thioflavine T interaction with synthetic Alzheimer's disease beta-amyloid peptides: detection of amyloid aggregation in solution, *Protein Sci. 2*, 404−410.
18. Yoshiike, Y., Tanemura, K., Murayama, O., Akagi, T., Murayama, M., Sato, S., Sun, X., Tanaka, N., and Takashima, A. (2001) New insights on how metals disrupt amyloid beta-aggregation and their effects on amyloid-beta cytotoxicity, *J. Biol. Chem. 276*, 32293−32299.
19. Libich, D. S., Hill, C. M., Bates, I. R., Hallett, F. R., Armstrong, S., Siemiarczuk, A., and Harauz, G. (2003) Interaction of the 18.5-kD isoform of myelin basic protein with Ca^{2+}-calmodulin: effects of deimination assessed by intrinsic Trp fluorescence spectroscopy, dynamic light scattering, and circular dichroism, *Protein Sci. 12*, 1507−1521.
20. Hertel, C., Terzi, E., Hauser, N., Jakob-Rotne, R., Seelig, J., and Kemp, J. A. (1997) Inhibition of the electrostatic interaction between beta-amyloid peptide and membranes prevents beta-amyloid-induced toxicity, *Proc. Natl. Acad. Sci. U.S.A. 94*, 9412−9416.
21. Weiser, H. B. (1933) *Inorganic Colloid Chemistry*, pp 21−57, John Wiley & sons, New York.
22. Lv, H., Zhang, S., Wang, B., Cui, S., and Yan, J. (2006) Toxicity of cationic lipids and cationic polymers in gene delivery, *J. Controlled Release 114*, 100−109.
23. Walton, J., Beeson, P. B., and Scott, R. B. (1986) *The Oxford Companion to Medicine*, Oxford University Press, London, UK.
24. Kanska, U., and Boratynski, J. (2002) Thermal glycation of proteins by D-glucose and D-fructose, *Arch. Immunol. Ther. Exp. 50*, 61−66.
25. Abraham, E. C., Cherian, M., and Smith, J. B. (1994) Site selectivity in the glycation of alpha A- and alpha B-crystallins by glucose, *Biochem. Biophys. Res. Commun. 201*, 1451−1456.
26. Roth, G. J., Stanford, N., and Majerus, P. W. (1975) Acetylation of prostaglandin synthase by aspirin, *Proc. Natl. Acad. Sci. U.S.A. 72*, 3073−3076.
27. Xu, A. S. L., Macdonald, J. M., Labotka, R. J., and London, R. E. (1999) NMR study of the sites of human hemoglobin acetylated by aspirin, *Biochim. Biophys. Acta 1432*, 333−349.
28. Etminan, M., Gill, S., and Samii, A. (2003) Effect of non-steroidal anti-inflammatory drugs on risk of Alzheimer's disease: systematic review and meta-analysis of observational studies, *BMJ 327*, 128.
29. Black, S. D., and Mould, D. R. (1991) Development of hydrophobicity parameters to analyze proteins which bear post- or cotranslational modifications, *Anal. Biochem. 193*, 72−82.
30. Jacobs, S. A., and Khorasanizadeh, S. (2002) Structure of HP1 chromodomain bound to a lysine 9-methylated histone H3 tail, *Science 295*, 2080−2083.
31. Gallivan, J. P., and Dougherty, D. A. (1999) Cation-pi interactions in structural biology, *Proc. Natl. Acad. Sci. U.S.A. 96*, 9459−9464.
32. Hardy, J., and Selkoe, D. J. (2002) The amyloid hypothesis of Alzheimer's disease: progress and problems on the road to therapeutics, *Science 297*, 353−356.
33. Caughey, B., and Lansbury, P. T. (2003) Protofibrils, pores, fibrils, and neurodegeneration: separating the responsible protein aggregates from the innocent bystanders, *Annu. Rev. Neurosci. 26*, 267−298.
34. Kirkitadze, M. D., Bitan, G., and Teplow, D. B. (2002) Paradigm shifts in Alzheimer's disease and other neurodegenerative disorders: the emerging role of oligomeric assemblies, *J. Neurosci. Res. 69*, 567−577.

BI700455C